A Coupled Approach to the Design Space Exploration of Nuclear Thermal Propulsion Systems

Victor L. Petitgenet[*], Christopher D. Roper[*], David Shalat[*], Andrew Yatsko[†], and Dmitri N. Mavris[‡]
Georgia Institute of Technology School of Aerospace Engineering, Atlanta, GA, 30332, USA

Matt Krecicki[§], and Dan Kotlyar[¶]
Georgia Institute of Technology School of Nuclear and Radiological Engineering, Atlanta, GA, 30332, USA

Nuclear Thermal Propulsion (NTP) is identified as one of the preferred propulsion technologies for future manned missions to Mars and other interplanetary destinations. NTP systems can improve the returns and mitigate the risks of such missions by reducing travel time and improving payload capacity as compared to traditional chemical propulsion systems. Due to the complexity and tightly coupled nature of the nuclear reactor and surrounding NTP subsystems, the traditional decoupled approach to NTP system analysis is inadequate. A new approach is needed to enable a high-fidelity design space exploration exercise for NTP systems. The approach outlined in this paper will address an integrated model of the reactor and supporting subsystems. This model, along with the incorporation of Design of Experiments and Surrogate Modeling, will allow for the exploration of the performance of a large number of NTP system designs with respect to metrics such as specific impulse and thrust to weight ratio. The subsystems analysis is handled by Numerical Propulsion Systems Simulation (NPSS) while reactor modeling is conducted using various numerical codes. This paper proposes and demonstrates a coupled design space exploration approach for NTP systems and uses these findings to consider vehicle-level implications.

I. Introduction

Nuclear powered space vehicles have been a technology of interest to the Atomic Energy Commission beginning in 1951 [1]. Research in this time period paved a roadmap for integrating nuclear power with propulsion technologies for in-space propulsion applications, a concept known as Nuclear Thermal Propulsion (NTP). The recent NASA Design Reference Architecture (DRA) 5.0 report identified NTP as the most favorable propulsion technology for future manned Mars missions [2]. NTP is favored due to its combination of high specific impulse, as compared to chemical propulsion systems, while providing improved performance with regard to thrust output and thrust to weight ratio, as compared to alternatives such as ion thrusters. As a part of early studies of NTP systems, throughout the 1960's, many NTP systems were researched and developed. This involved programs such as NERVA, Kiwi, and Rover which, in part, focused their research on the study of reactor core design [3]. Some of these efforts culminated in the development and on-Earth testing of a full NTP system in order to determine feasibility for missions such as manned missions to Mars.

II. Background and Motivation

In 2018, the National Space Exploration Campaign highlighted critical components and opportunities for spacecraft technologies that will facilitate future manned and unmanned missions. The National Space Exploration Campaign plans to build and expand upon NASA's Mars Exploration Program (MEP) missions to further the United States' leadership on Mars with subsequent crew missions in the near future [4]. With early design studies of such interplanetary manned missions ongoing, there exists a need for supporting such technical analyses with the tools and capabilities required to enable successful decision making. An example of such a capability is design space exploration, a practice which enables the analysis of design alternatives before pursuing an implementation [5]. As a

[*] Graduate Researcher, Aerospace Systems Design Laboratory, Student Member AIAA
[†] Research Engineer, Aerospace Systems Design Laboratory, Senior Member AIAA
[‡] Boeing Regents Professor of Advanced Aerospace Systems Analysis, Fellow AIAA
[§] Graduate Research Assistant Computational Reactor Engineering Laboratory
[¶] Assistant Professor

part of NASA's initiative to pursue crewed missions to the Martian surface, this paper provides a methodology for the coupled analysis of an NTP system by leveraging subject matter expertise from nuclear and aerospace engineering. This methodology is then implemented to demonstrate a design space exploration capability for NTP systems.

Traditionally, NTP sub-system and reactor core analyses have been treated as decoupled [3]. This has been the case due to the highly interdisciplinary nature of an NTP system which requires combined knowledge of aerospace propulsion system analysis and design as well as nuclear reactor analysis and design. Although there can be certain benefits brought by isolating and analyzing subsystems on an individual basis, a coupled environment linking the analysis of the supporting NTP subsystems to that of the nuclear reactor is required to unlock the capability of parametric, rapid design space exploration. Such an approach is necessary due to the sensitivity of reactor performance to inlet conditions driven by the upstream subsystems as demonstrated by previous work in the field [6].

This paper details a coupled approach which leverages tools to support the high-fidelity analysis and design of the NTP system as a unified system. The appropriate environment is created using Numerical Propulsion System Simulation (NPSS) which provides support for the high-fidelity analysis of the supporting NTP subsystems as well as for the integration of a custom reactor module. The reactor module consists of a combination of reactor analysis codes, from Georgia Tech's Nuclear and Radiological Engineering Department. This paper details the development of this approach as well as resulting capabilities and gives insight regarding the vehicle level implications of the design space exploration of the propulsion system.

III. Coupled Approach Methodology

A. Proposed Methodology Overview

In order to approach the design space exploration exercise in a coupled manner, the methodology developed and implemented as part of this paper leverages a cooperative effort between two research departments. The team from Georgia Tech's Aerospace Systems Design Lab (ASDL) will leverage experience related to the modelling of aerospace systems while the researchers from Georgia Tech's Nuclear and Radiological Engineering Department (NRE) will utilize knowledge and expertise related to the high-fidelity modelling of nuclear reactors.

The methodology proposed as part of this approach is notionally represented in Fig. 1. A Bimodal Nuclear Thermal Rocket (BNTR) model created within NPSS is utilized as the baseline model and system architecture. In order to transform this model into a coupled model, in-house NRE codes for calculation of the neutronics and thermal hydraulics are utilized to generate a surrogate of the reactor model based on a pre-defined set of boundary constraints to the system's inlet and outlet conditions. This surrogate is then implemented as an NPSS module within the BNTR model in the form of an interpolable lookup table.

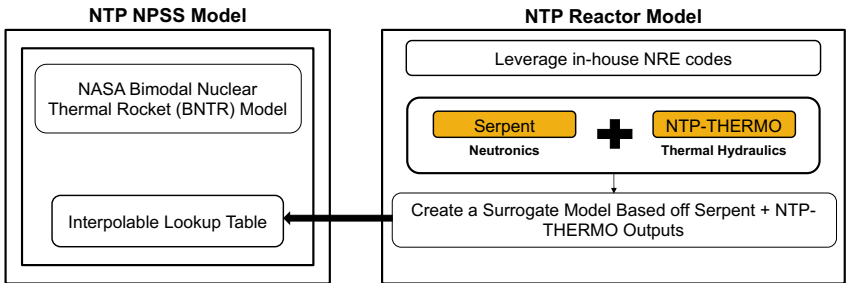

Fig. 1 Coupled approach outline.

The architecture utilized for the BNTR model consists of a solid core reactor with a CERMET low-enriched uranium fuel. NTP systems utilizing low-enriched fuel have been identified as the most promising path for developing NTP systems due to their potential for reducing program development costs and compliance with US government policy [7]. As such, due to feasibility constraints for a particle/pebble bed reactor when utilizing a low-enriched fuel, the core type consists of NERVA-like fuel elements and solid moderator elements. The reactor is utilized as the heat source for a closed expander cycle engine consuming cryogenic hydrogen propellant, and it is assumed that passive radiation shielding will be used throughout the system. Although the methodology detailed in this paper is flexible to any NTP system architecture, this paper is focused on the demonstration of this methodology for a single system architecture.

B. Tools & Modelling - NPSS

As discussed previously, there is a lack of an existing computational framework which allows for the coupled analysis of an NTP system. As a result of this, the first step in moving towards the design space exploration of an NTP system required the creation of such a suitable environment. To accomplish this, this paper selected NPSS as the framework which supports the modelling of both the reactor system as well as supporting NTP systems. NPSS is an object-oriented, multi-physics, engineering design and simulation environment that enables development, collaboration and seamless integration of system models [8]. Areas of application within aerospace include engine performance models for aircraft propulsion, thermodynamic system analysis, and various rocket propulsion cycles. The software was selected due to high levels of expertise within ASDL for the analysis of propulsion systems using NPSS, NPSS's flexibility to support the high-fidelity modelling of traditional propulsion subsystems such as turbomachinery, and also customizability to define a custom module to support the modelling of the reactor system. In addition to this, the NPSS solver allows the user to solve multiple problems with the same model by defining independent and dependent variables as well as constraints.

C. Tools & Modelling - Reactor Core

SERPENT is a versatile three-dimensional Monte Carlo particle transport code developed at the VTT Technical Research Centre of Finland. Serpent allows for the modelling of complex irregular 3D geometries, which is an extremely advantageous feature for advanced NTP designs. The code achieves more efficient CPU time performance due to the code's implementation of Woodcock delta-tracking [9] of particles. In our current study, ENDF/B-VII.0 evaluated data library was used [10]. Recent releases of the code have included coupled neutron and gamma transport capabilities [11]. These capabilities were enabled to account for the gamma heating effect on the shape of the axial power profiles used in T/H sub-channel analysis. The post processing of SERPENT output files was conducted using the *serpentTools* python package [12].

The thermal hydraulic solution was calculated utilizing the NTP-THERMO code, which was developed internally by the Computational Reactor Engineering Group at Georgia Tech [6][13]. NTP-THERMO relies on the equivalent annulus approximation to solve the radial conduction problem within the fuel element and a 1.5D conduction-convection solution. All material properties are temperature dependent. Additionally, the hydrogen coolant are temperature and pressure dependent.

A finite difference model was used to solve the steady-state mesh-based resistance network. The code includes an implementation of a numerical solution to the radial conduction problem. This approach was adopted to provide an accurate solution of the heat transfer coefficient correlation which depends on the fuel surface temperature and bulk coolant temperature. The NASA Glenn research center developed several Nusselt number correlations for gas flowing through a heated pipe. [14] Taylor's correlation was adopted to solve the fuel element flow channel, and Petukhov's correlation was used to solve the moderator element flow channels. A detailed description of this solution scheme can be found in previously published literature [6].

Since the fuel and moderator elements are in direct contact with each other there is some heat transfer from the hot fuel elements (FE) to the cold moderator elements (ME). This is a difficult problem to solve since the inlet conditions of the fuel element are dependent upon the outlet conditions of the moderator element. In order solve this issue the problem was divided into three separate problems. The converged solution is obtained via the iterative computational scheme presented in Fig. 2. The inlet conditions to the supply channel (MES) are well known and not dependent on the moderator outlet or fuel outlet conditions, therefore they are held constant throughout the solution. The outlet conditions of the MES are set as the inlet conditions to the return channel (MER). The FE is solved independently to obtain the fuel centerline temperature axial distributions, which are then also used in the solution of the return channel as the wall boundary conditions. This loop is repeated until the wall boundary temperature has converged [6][13].

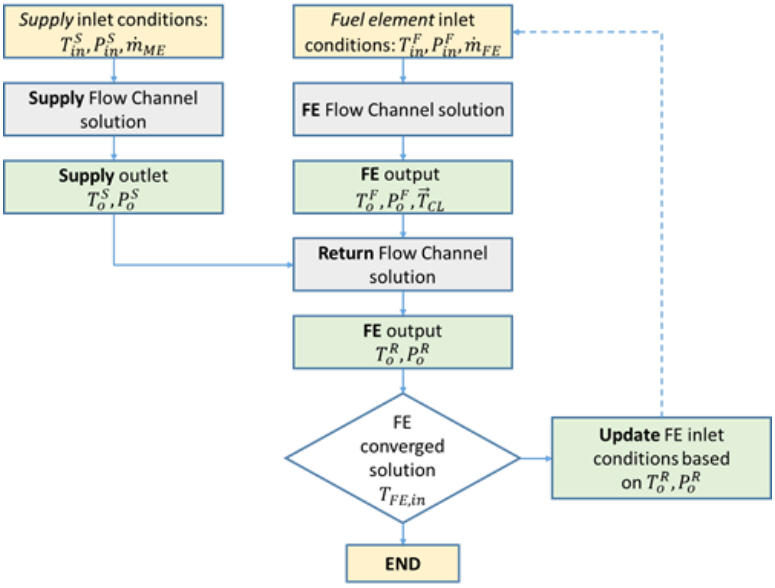

Fig. 2 Fuel element to moderator element heat transfer solution scheme [13].

The resulting axial power profiles from the SERPENT model are presented in Fig. 3. Axially, the model was divided into 120 nodes/layers in the SERPENT model in order to provide a detailed power profile. Both neutron and photon energy deposition are accounted for in the analysis. Previous research conducted at Georgia Tech has demonstrated that the axial power shape has a significant effect on the maximum allowable power density of a given core. The configuration presented in this work was chosen from a predetermined promising design space region [6].

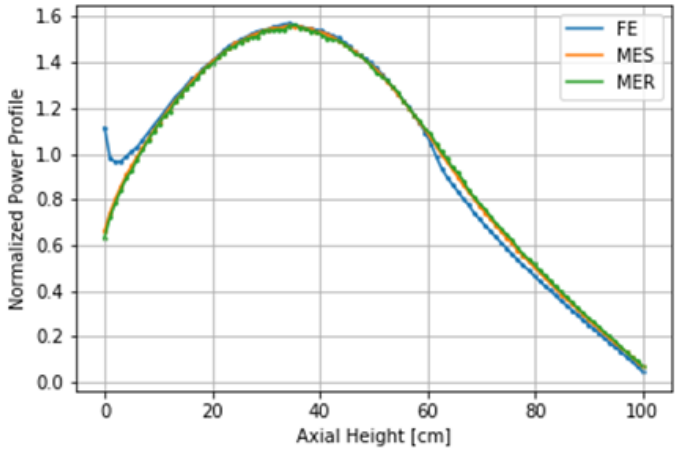

Fig. 3 SERPENT calculated axial power profiles.

The SERPENT calculated power profile was then implemented into the NTP-THERMO sequence. The primary purpose of NTP-THERMO is to calculate the exiting gas conditions of the fuel elements and moderator elements, while also determining the margin to failure of each element. The bulk coolant temperature for the average channel is presented in Fig. 4. An axial height of 0 cm represents the top of the reactor core towards the axial reflector (propellant inlet), and an axial height of 100 cm represents the bottom of the core (propellant exit). The majority of bulk coolant temperature increase occurs within the fuel elements, this result is expected as over 94% of the total reactor power is deposited in the fuel. The moderator supply and return channel temperature are shown to be continuous, however there is a discontinuity between the fuel inlet and moderator return temperature.

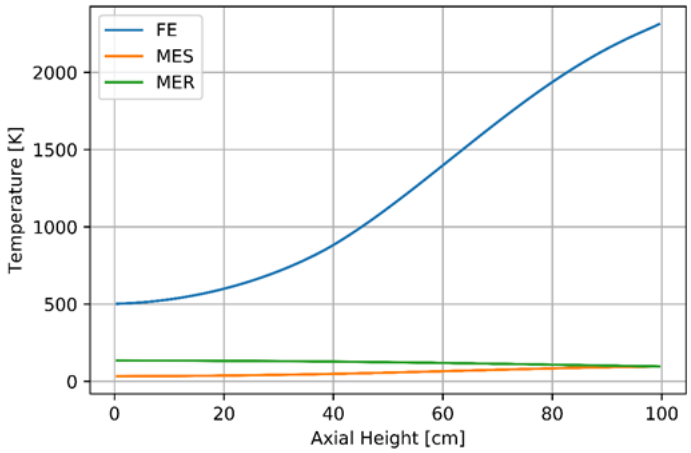

Fig. 4 Bulk coolant temperature profile.

The Graph-TIT-E friction factor correlation was chosen as it was within the accepted range of Reynolds numbers and yielded the largest pressure drops across each channel. Only friction and acceleration losses are considered in this analysis as gravitational losses can be neglected and the internal cooled fuel elements suffer no form losses across the flow path.

One of the most critical aspects of the NTP core design is maintaining thermal margins in the fuel element. The maximum temperature of the fuel element and each region's thermal limit is presented in Fig. 5. The maximum fuel temperature is plotted by the blue curve and measured on the left-hand y-axis label. The margin to fuel-element thermal failure is plotted in orange and measured on the right-hand y-axis label. The dashed grey lines represent the maximum allowable temperature in that region of the fuel element. The dashed red line represents where the fuel transitions from Mo-UN to Mo/W-UN, as such the maximum allowable temperature increases. The same analysis is presented for the ZrH_x sleeve in the supply channel in Fig. 6. However, this figure presents simpler trends as the maximum temperature across the entire element is the same. An important observation should be made that the margin to element failure is always positive across the entire fuel and moderator element.

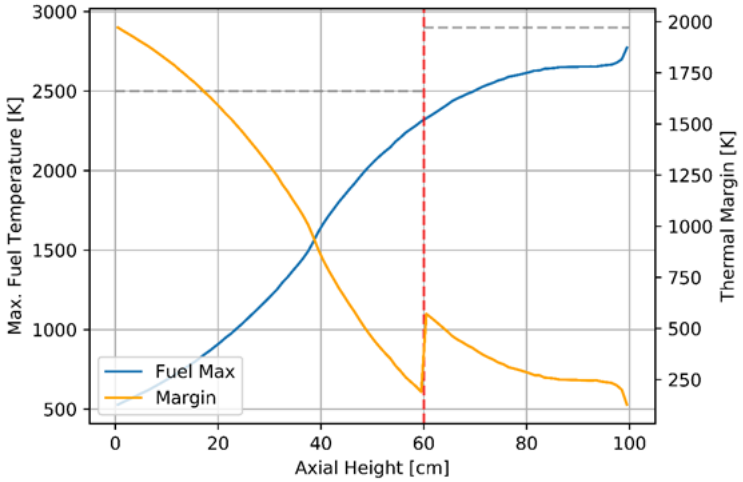

Fig. 5 Fuel thermal margins.

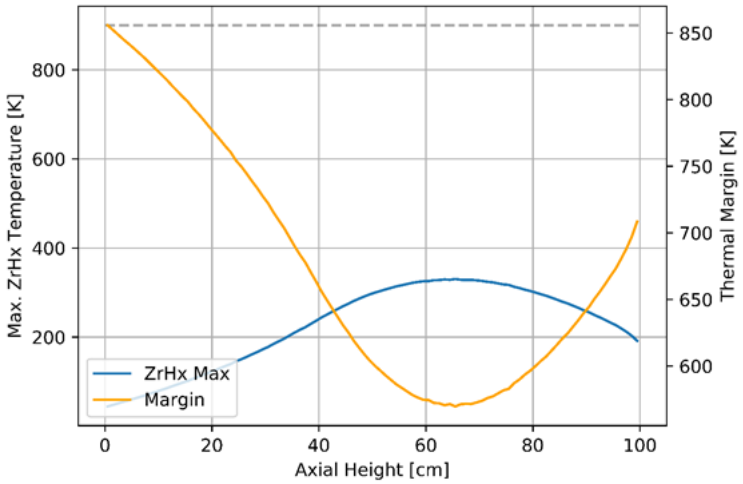

Fig. 6 ZrH_x thermal margins.

D. Boundary Constraints

As part of achieving the coupling between NTP subsystem models and a high-fidelity reactor model within NPSS, it was first necessary to generate a series of boundary conditions imposed on the reactor system. These boundary conditions establish a range of expected conditions that the reactor must operate within in order to meet the established overall system goals and allow for the creation of a lookup table to model the reactor performance. The values needed to generate the lookup table are listed in Table 1. Since identifying the boundary conditions to the reactor is necessary to generate the lookup table, it must precede the creation of the higher-fidelity NTP model within NPSS. Thus, to favor a more straightforward calculation process, this method relies on utilizing a simplified flow cycle as well as a set of simplifying assumptions. These simplifications entail that the results from this process are not entirely reflective of the boundary conditions of a real system. Despite this fact, by utilizing sufficiently conservative assumptions, it is possible to create a range of boundary conditions that are reflective of a real reactor system.

Table 1 Variable Ranges Required to Generate Lookup Table

Variable Name	Units
Total Reactor Power	MW
Mass Flow Rate to Moderator Elements	kg/s
Mass Flow Rate to Fuel Elements	kg/s
Inlet Temperature to Moderator Elements	K
Inlet Pressure to Moderator Elements	kPa
Inlet Temperature to Fuel Elements	K
Inlet Pressure to Fuel Elements	kPa

The procedure begins by identifying a range of targets for thrust and specific impulse as shown in Table 2. These targets are based on the NASA Mars DRA-5.0 requirements [2]. In addition to these targets, ranges for inner reactor chamber pressures and temperatures are defined as shown in

Table 3. These ranges constrain the operating envelope of the NTP system and are based off realistic inner reactor pressure chamber conditions taken from [15].

Table 2 System Level Performance Targets

Parameter	Target Value
Thrust (klb_f)	24-26
Specific Impulse (s)	≥850

Table 3 Pressure Chamber Temperature and Pressure Ranges

Parameter	Range
Inner Reactor Chamber Temperature (K)	2,500 - 3,333
Inner Reactor Chamber Pressure (kPa)	6,000 - 9,600

Using these values and making assumptions regarding nozzle geometry and gas properties from literature values, the inner reactor chamber conditions can be utilized to solve for the required mass flow rate to meet the thrust target for a combination of chamber temperature and pressure. With the matrix of mass flow rates solved for, dividing the mass flow rate by the thrust target gives the specific impulse of the system. In the case that the specific impulse target is not met, the mass flow rate value is defaulted to zero and not used for subsequent analysis. The result of this process is a range of temperatures, pressures, and mass flow rates at the inner reactor pressure vessel exit that allow for both the thrust and specific impulse targets to be met.

The next step of this analysis is to calculate the range of boundary conditions to the reactor inlet. The range of these inlet conditions largely depends on the turbomachinery characteristics leading to the inner reactor chamber. First, a tank temperature and pressure are established based on literature values for similar systems [16], these are treated as constant for the purposes of this calculation. Sweeps are then defined for three key turbomachinery characteristics as detailed in Table 4 based on literature values [15].

Table 4 Ranges for Calculating Reactor Inlet Boundary Conditions

Parameter	Lower Bound	Upper Bound
Pump Pressure Ratio	40	80
Pump Efficiency	0.6	0.8
Turbine Efficiency	0.7	0.9

With these ranges defined, the next step is to walk through the simplified cycle analysis of the propulsion system to arrive at the reactor inlet conditions for each of the different combination of characteristics and for each mass flow rate which allows for the thrust target to be met as detailed previously.

Performing the cycle analysis for different combinations of allowable mass flow rates and turbomachinery characteristics allows for recording the required parameters to generate the lookup table for each iteration. The bounds are found by retaining the respective minimum and maximum for each variable across all iterations. To account for the simplifications and assumptions made in obtaining these values, the bounds are expanded by respectively subtracting and adding 10% of the average value for each bound to the respective lower and upper limits. According to this calculation procedure the reactor outlet boundary condition results for the reactor outlet are summarized in Table 5 and the reactor inlet boundary condition are summarized in

Table **6**. These bounds were then utilized to generate the multidimensional lookup table.

Table 5 Reactor Outlet Boundary Conditions

Parameter	Lower Bound	Upper Bound
Fuel Elements Outlet Temperature (K)	2,261	3,628
Fuel Elements Outlet Pressure (kPa)	5,232	10,119

Table 6 Reactor Inlet Boundary Conditions

Parameter	Lower Bound	Upper Bound
Total Reactor Power (MW)	411	647
Mass Flow Rate to Moderator Elements (kg/s)	2.27	9.53
Mass Flow Rate to Fuel Elements (kg/s)	9.53	14.97
Inlet Temperature to Moderator Elements (K)	25	82
Inlet Pressure to Moderator Elements (kPa)	7,970	20,160
Inlet Temperature to Fuel Elements (K)	243	413
Inlet Pressure to Fuel Elements (kPa)	5,595	13,402

E. NTP NPSS Model

At the first step of creating a fully integrated model is recreating the NTP system flow cycle within NPSS. A flow diagram for a closed expander cycle NTP system is shown in Fig. 7.

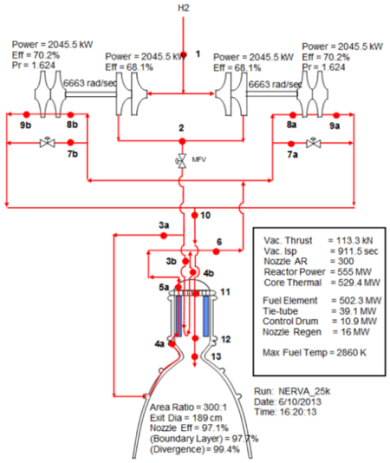

Fig. 7 Closed expander cycle NTP system [15].

With the choice of a flow cycle completed, the chosen cycle was then recreated within NPSS using a combination of built in and in-house developed component modules according to the notional block diagram shown in Fig. 8. With the model created, NPSS can iterate upon the system to calculate the system performance parameters such as thrust and specific impulse.

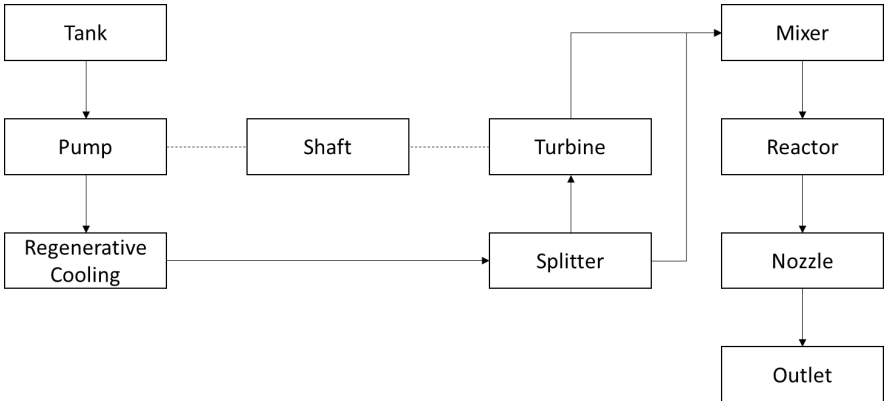

Fig. 8 NTP Closed expander cycle block Diagram.

While the built-in NPSS modules allow for the modelling of traditional rocket turbomachinery elements such as pump, pipes, and turbine, the NPSS environment does not allow for the modelling of the reactor element at sufficient fidelity. It is at this stage that our project aims to create and integrate a reactor module within the NPSS environment.

After defining boundary constraints and receiving the interpolable lookup table from NRE, this information was integrated into the BNTR model to result in the final high-fidelity model. To do this, a new reactor element was created which performs thermodynamic and mass analysis based on the interpolable lookup table. Reactor design decisions resulted from extensive research completed within the NRE department, and while not a comprehensive list, some key reactor elements for the selected design are listed below in Table 7.

Table 7 Key Reactor Parameters

Parameter	Value
Number of Fuel Elements	367
Fuel Enrichment	19.75 (wt%)
Number of Moderator Elements	588
Core Height	100 (cm)
Axial Split	0.4
Radial Power Peaking Factor	1.08
Cold End Maximum Fuel Temperature	2500 (K)
Hot End Maximum Fuel Temperature	2900 (K)
ZrH_x Maximum Temperature	900 (K)

Fig. 9 depicts a detailed cross section of the reactor core radial configuration. This consists of a graphite sleeve surrounding an active core, followed by a void, a zirconium carbide insulator, an Al-2024 inner pressure vessel, a beryllium radial reflector with boron carbide control drums embedded within, and an Al-2024 outer pressure vessel.

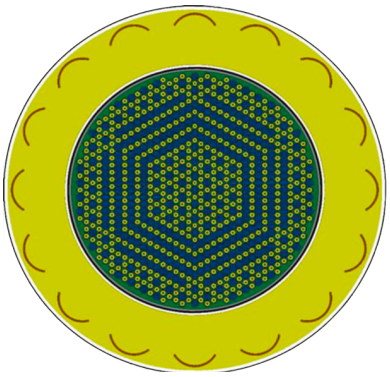

Fig. 9 Reactor core configuration [13].

This reactor design was passed to the NRE reactor analysis codes discussed previously to generate the multi-dimensional look up table. Due to extreme computational costs, the lookup table was generated using a grid spacing who's spacing was determined from previous sensitivity studies. Specific input parameters to the lookup table are listed in Table 1. A combination of these inputs resulted in 6705 unique cases and calculations yielded the following output parameters: fuel element exit gas temperature, maximum centerline fuel temperature, fuel element outlet pressure, fuel element power, moderator element supply power, moderator element return power, reflector power, moderator element outlet temperature, moderator element outlet pressure, fuel melting margin, ZrH_x melting margin, limiting fuel node height, power conducted to moderator, reactor mass, core height, number of fuel elements, and core ID number. Finally, this table is included into the reactor module as a map which then receives inputs from other modules, model inputs, and internally calculated values. The module then outputs interpolated values from the lookup table to be used by the rest of the NPSS model.

In order to calculate the system's thrust to weight ratio, an additional user function was created and integrated into the NPSS model to calculate the size and weight of the overall system including the size and weight of each major component. A variety of sources and methods were used to provide a conceptual design level understanding of the component sizes and weights. The output of the NPSS model provides the necessary inputs into the user function to calculate sizes and weights.

F. Design of Experiments and Surrogate Modelling

While the incorporation of the reactor model in the form of a surrogate model serves to reduce the overall complexity, the analysis of the overall NPSS model remains highly computationally intensive with a single run taking around 6 seconds. While this computation time is hardly problematic for a single run or a handful of runs, it becomes problematic when there exists the need to investigate tens of thousands of designs such as for a design space exploration exercise. Circumventing this challenge requires the implementation of surrogate modeling. Creating the surrogate models consists of three steps. First, a Design of Experiments (DoE) is conducted such that the inputs to the

model are intelligently designed in order to extract a maximum amount of information with a minimum required computational effort. Next, this DoE consisting of a series of discrete designs is fed to the NPSS model. Once this DoE has run, the final step consists of using the outputs of the DoE to generate surrogate models or metamodels of the desired outputs as a function of the design variables. With the surrogates created, designs can be investigated nearly instantaneously and exploring tens or hundreds of thousands of designs within the design space becomes a manageable task.

For the purposes of this paper, the DoE was created based of a combination of a Latin Hypercube design to cover the interior of the design space, and a Face Centered Central Composite design to cover the edges of the space. This combination allowed for a complete exploration of the design space with 20,000 cases allocated to the Latin Hypercube design and 513 cases allocated to the Face Centered Central Composite design. The input variable ranges for this DoE are shown in Table 8. The ranges used for this DoE come from the boundary calculation exercise discussed previously and were updated using results from a preliminary DoE run where it was found that high reactor powers led to an infeasible system. This DoE was created and run in ModelCenter 12.0 to automate the process of generating input files for NPSS and reading data from NPSS output files for each of the 20,513 runs. The total computational time for running this DoE amounted to approximately 34 hours.

Table 8 Design Variables Ranges for DoE

Design Variable	Minimum	Maximum
Thrust (lbf)	24,000	26,000
Reactor Power (MW)	400	450
Nozzle Area Ratio	150	350
Tank Temperature (K)	19.9	20.59
Tank Pressure (MPa)	0.145	0.159
Reactor Inlet Pressure (psi)	1450	1600
Compressor Efficiency	0.6	0.8
Turbine Efficiency	0.7	0.9
Shaft Speed (rpm)	20,000	30,000

The results from this DoE were then imported into Excel in order to filter results before the creation of surrogate models. Filtering is performed namely to remove cases for which the NPSS model failed to converge. It should be noted that any cases which failed in ModelCenter are automatically filtered since they are not included in the DoE results. Fig. 10 provides the breakdown of filtered and retained cases highlighting that 95% of the original 20,513 cases generated as part of the DoE were used for surrogate model creation.

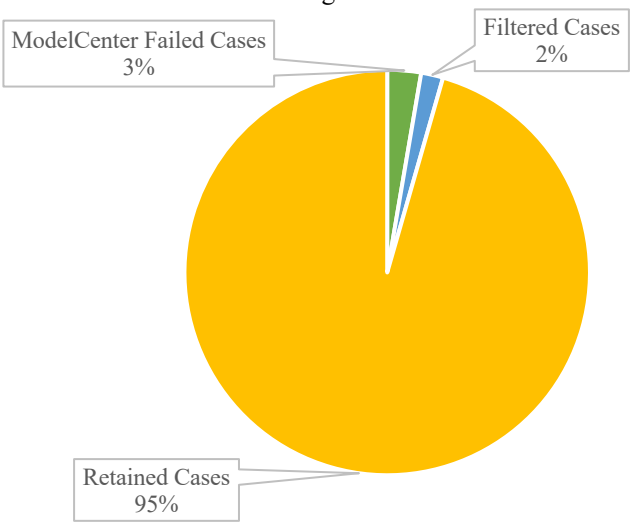

Fig. 10 DoE output breakdown.

Using the filtered DoE results, surrogate models are generated for certain responses of interests in JMP. As highlighted in Table 9, which summarizes the characteristics of the surrogate models generated as part of this project, a mix of Linear Regressions and Neural Networks are used to fit a surrogate to the response. This choice is driven by the R^2

value, if fitting a model using a linear regression fails to attain an acceptable R^2, a Neural Network is then used. With these surrogate models generated, prediction formulae can then be saved within JMP to allow for the near-instantaneous evaluation of the system's responses as functions of the design variables. This capability allows for the exploration of the design space for the NTP system in a real-time manner.

Table 9 Summary of Surrogate Models

Response	Surrogate Type	R^2
Thrust Output	Linear Regression	1.0000
Specific Impulse	Neural Network	0.9993
Fuel Melting Margin	Neural Network	0.9985
ZrHx Melting Margin	Linear Regression	0.9987
System Weight	Neural Network	0.9822
Fuel Element Outlet Temperature	Linear Regression	0.9975
System Length	Linear Regression	0.9992
System Radial Envelope	Linear Regression	0.9999
Nozzle Exit Diameter	Linear Regression	0.9999
Fuel Element Mass Flow Rate	Linear Regression	0.9955
System Thrust to Weight Ratio	Linear Regression	0.9938

IV. Results

G. Prediction Profiler

Leveraging the surrogate models discussed previously, a prediction profiler of the responses versus the design variables can be generated within JMP. The prediction profiler displays the partial derivative of the responses with respect to each design variable. In addition, the prediction profiler allows the user to make real-time adjustments to the design variables and consult the impact on the responses. Fig. 11 displays the prediction profiler created for the NTP system. The prediction profiler shows the responses on the y-axis and the design variables on the x-axis. The plot for each combination characterizes the nature of the system's response to a change in the corresponding design variable.

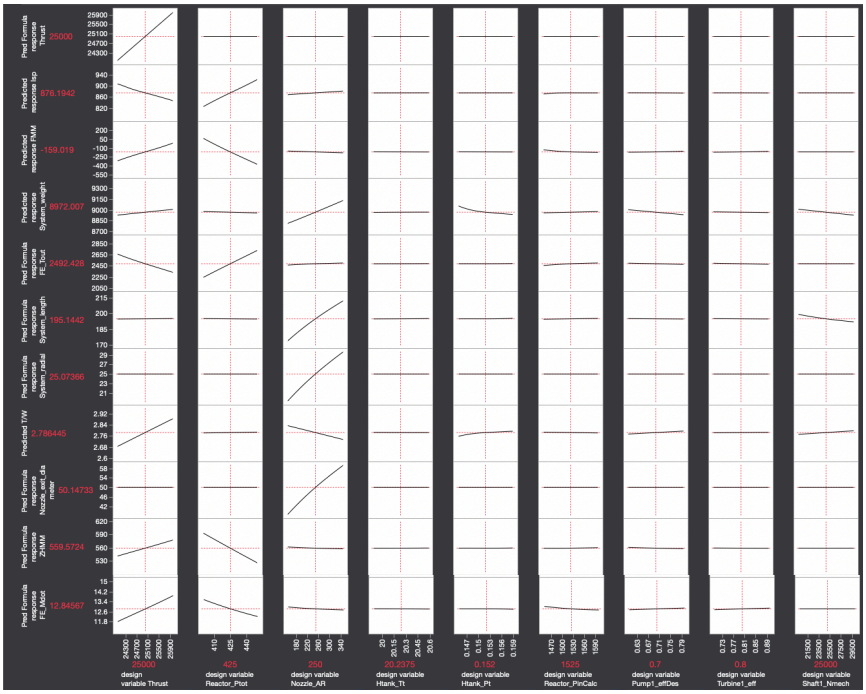

Fig. 11 JMP prediction profiler for the NTP NPSS model.

One application of the prediction profiler is to use the trends it demonstrates to analyze the extent to which the surrogate models capture the behavior of a real system. Fig. 12 highlights one such analysis showing the surrogate's prediction for weight as a function of thrust. The results from this plot highlights a positively correlated linear trend as established by literature results for liquid rocket engines [17][18]. Although Fig. 12 does show a positive trend, this trend is relatively weak compared to trends found in literature values [17][18]. This is due to the fact that since a single reactor configuration is implemented within the lookup table, between 64.1% to 71.4% of the total system's weight is constant since both the reactor and "Shadow" shielding weight are considered constant.

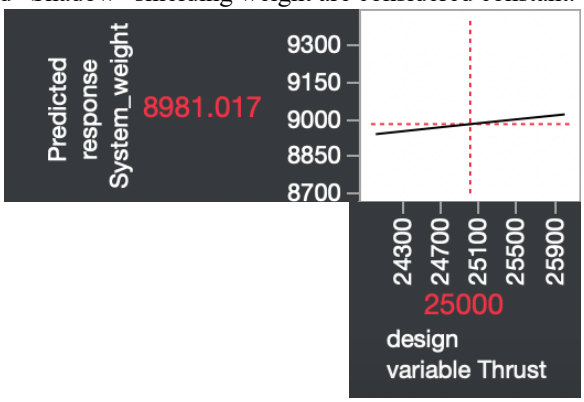

Fig. 12 System weight as a function of thrust output.

Another such analysis is presented in Fig. 13 where a positive correlation between specific impulse and the nozzle area ratio is predicted. This correlation also matches expected results from theory found in literature [19]. While this section discusses and compares certain trends to expectations from theory, it should be noted that the intent is not to calibrate or verify the findings from this paper to available literature values. Rather, the intent is to build confidence that the model reflects the behavior of a real system.

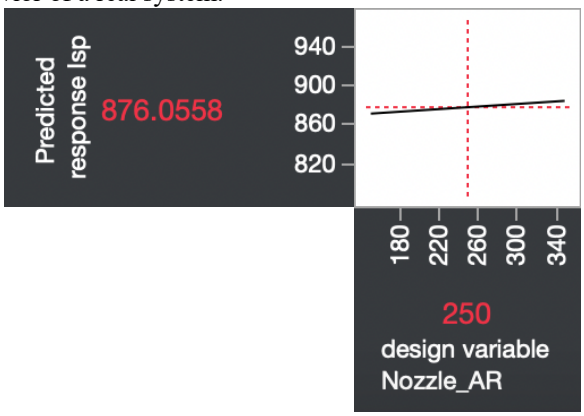

Fig. 13 Specific impulse as a function of nozzle area ratio.

In addition to allowing for the comparison of observed trends to literature values, the prediction profiler gives insight with regard to tradeoffs that exist within the multidimensional design space of the NTP system. One such tradeoff exists between T/W and specific impulse as shown in Fig. 14. As seen from the prediction profiler, while increasing the nozzle area ratio has the effect of increasing the specific impulse this comes at the cost of system T/W. Another such tradeoff exists between specific impulse and T/W with respect to the system's design thrust where a higher design thrust increases the system's T/W at the cost of specific impulse. This tradeoff is shown in Fig. 15.

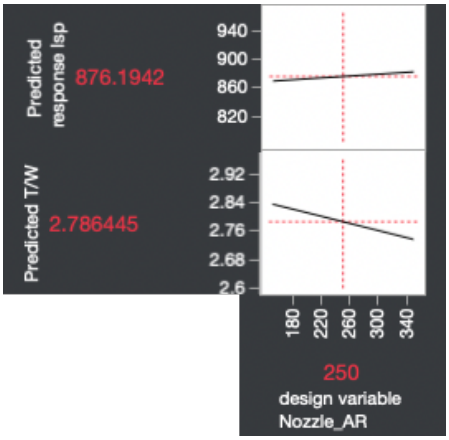

Fig. 14 T/W and specific impulse tradeoff with respect to nozzle area ratio.

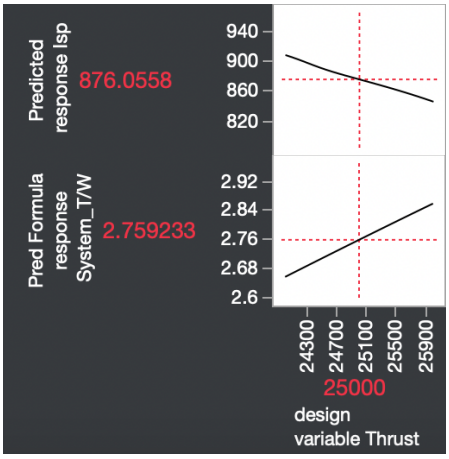

Fig. 15 T/W and Specific impulse tradeoff with respect to design thrust.

H. NTP System-Level Implications

The surrogate models also enable the capability to view the continuous, multidimensional design space of the NTP system in a manageable fashion. Fig. 16 shows this design space with respect to the design thrust and reactor power, although the same plot can be reproduced for any combination of design variables. Overlaid on this plot is the fuel melting margin (FMM) constraint shown as the green line with the unshaded region representing the feasible space. The FMM describes the difference between the maximum allowable fuel element temperature based on material properties and the fuel element operating temperature for a given NTP system design. For the purposes of this paper, based on subject matter expertise, the maximum allowable temperature was defined to be 200 K below melting temperature. As such, a negative FMM is deemed infeasible due to the potential for structural degradation of the system.

Also included are contours for T/W (placed at T/W=2.8) and ISP (placed at ISP=830 s) where the dotted side represent the increasing direction. As anticipated previously, the FMM is shown to significantly limit the feasible region of the design space as much of the space lies within the infeasible FMM region shaded in green. Fig. 16 serves to highlight the limitations placed on the design space by the FMM constraint. Namely, feasible designs are limited to using lower reactor powers which places an upper bound on the maximum attainable specific impulse for a feasible NTP system design. Additionally, the FMM places a lower bound on the system's design thrust level, where the

minimum feasible thrust, for the design used to generate this figure, is slightly higher than 24.5 klb_f which is consistent with the approximate thrust target set by the NASA Mars DRA 5.0 document.

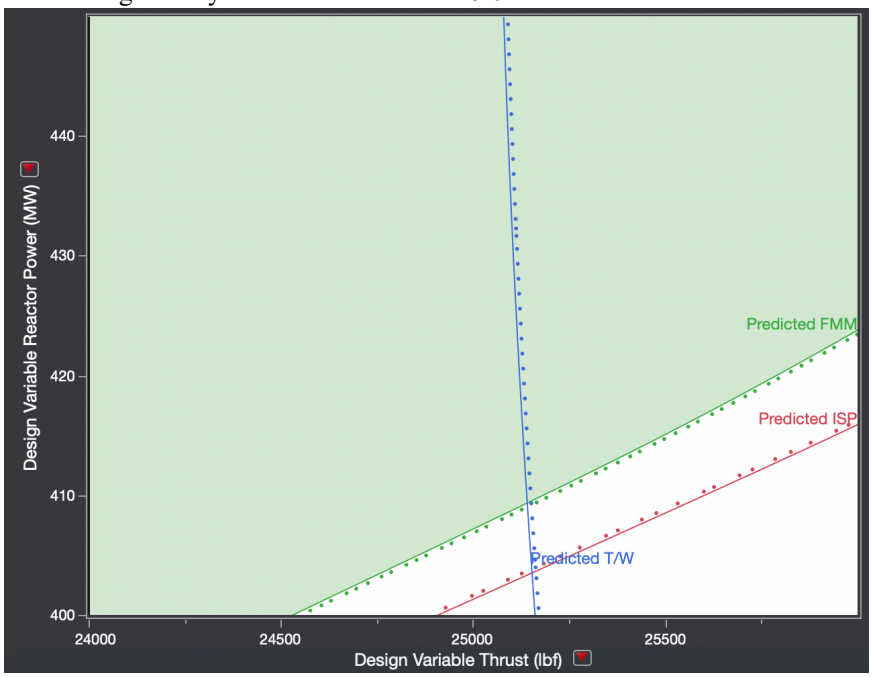

Fig. 16 NTP design space contour plot.

The feasible region of Fig. 16 also serves to provide insight regarding the design considerations of an NTP system. Firstly, as first remarked using the prediction profiler, the contour plot also indicates the presence of a tradeoff between T/W and specific impulse. Whereas the gradient of T/W points in the direction of increasing thrust, the gradient of specific impulse points in the direction of decreasing thrust. Thus, within the feasible region, the maximum T/W and specific impulse cannot be achieved simultaneously. As seen from the shaded region, the FMM constraint places an upper bound on the maximum reactor power that is well below the maximum value considered. This has the effect of restricting the maximum feasible specific impulse as well as T/W. Another key observation is that although the ZrH_x melting margin is also included as part of this contour plot, it does not constrain the design space.

I. Vehicle-Level Implications

While this paper has focused on establishing a methodology for the coupled design space exploration of NTP systems, the aim of this paper is not to consider this capability in a void. Rather, the aim is to lay out the methodology for developing such a capability and consider some of the more far-reaching insight provided by such a capability. An instance of this can be achieved by considering the vehicle-level implications of the NTP system design. To achieve this, a code was developed to size the propulsion stage of a hypothetical interplanetary transfer vehicle as described in Mars DRA 5.0. The propulsion stage architecture consists of three 25 klb_f NTP engines connected to an Aluminum-Lithium tank for cryogenic LH_2 as highlighted in Fig. 17.

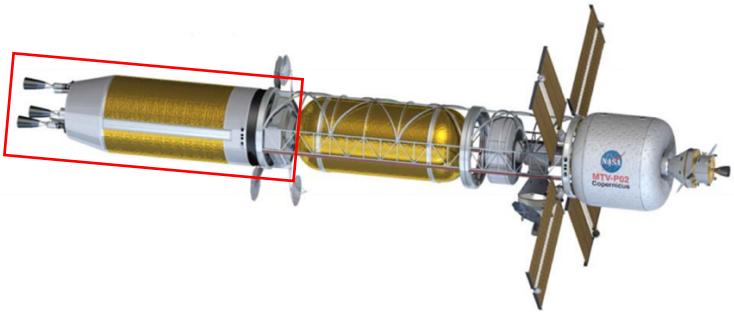

Fig. 17 Reference crewed mars transfer vehicle [2].

The propulsion stage also contains a Brayton-Cycle cryocooler and external crew radiation shielding. While the tank mass and engine mass are considered to be variable depending on the results of the stage sizing algorithm and NPSS model respectively, literature values are used to calculate the length and mass of auxiliary systems for the stage [4]. In addition, using data from [4], the tank mass (excluding external subsystems) is calculated as a function of its surface area. Using this information as well as the dynamic envelopes and mass constraints for a variety of heavy launch options as shown in Table 10, a constrained optimization algorithm is used to size the tank to maximize stage delta-v while adhering to the mass and dynamic envelope constraints.

Table 10 Launcher Mass and Diameter Constraints [20] [21]

Launcher	Mass Capacity to LEO (t)	Launch Vehicle Dynamic Envelope (m)
Starship	100	8.00
SLS Block 2	130	9.10

The algorithm assumes a retractable nozzle length of 2.16 m [4] and mounts the vehicle "upside-down" in the payload fairing with the engine nozzles pointing along the positive z-axis of the launch vehicle. It is also assumed that the tanks are filled with LH_2 on liftoff, and the mass of hydrogen propellant is calculated based on the tank volume and propellant density. With this sized vehicle, the ratio of dry mass to wet mass of the stage can be evaluated and combined with the engine specific impulse from the NPSS model to enable the code to calculate the stage delta-v based on the ideal rocket equation. The code is also capable of outputting a notional visual of the stage packed into the payload fairing of the launch vehicle as shown in Fig. 18.

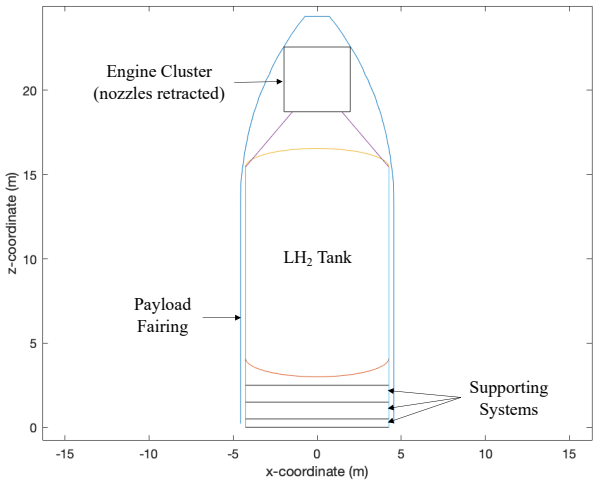

Fig. 18 Vehicle visualization from sizing code.

This vehicle sizing algorithm is used to analyze feasible designs from a set of 50,000 cases generated using the surrogate models with the results shown in Fig. 19 and Fig. 20. As seen in these figures, the behavior of the optimization algorithm causes clustering of the sized vehicles based on the nozzle area ratio. Furthermore, these figures highlight the fact that both launcher options are volume-constrained as opposed to mass-constrained which is expected due to the large proportion of the vehicle dedicated to LH_2. Comparing the resulting delta-v for both launch vehicles provides evidence that the larger dynamic envelope of SLS Block 2 allows for substantially greater delta-v.

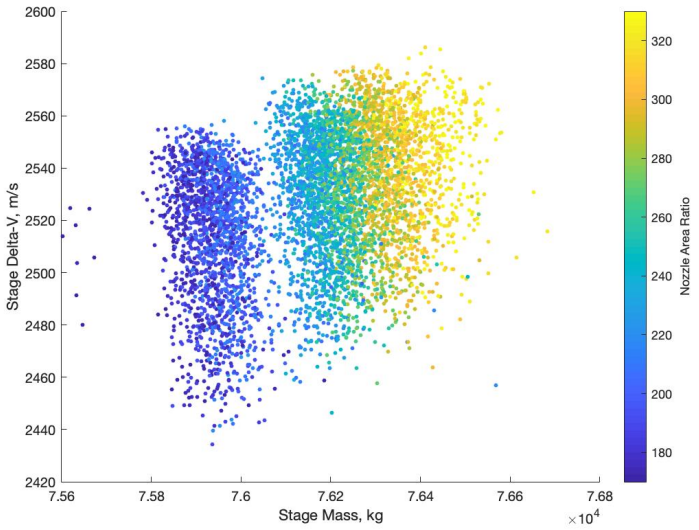

Fig. 19 Scatter plot of stage delta-v versus stage mass for Starship colored according to nozzle area ratio.

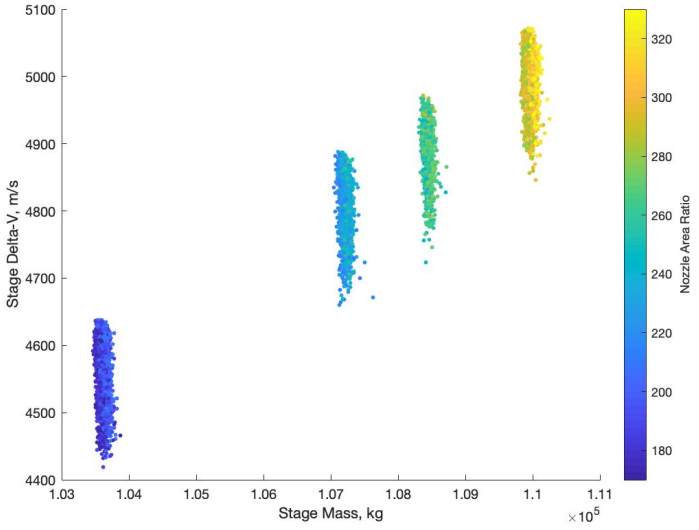

Fig. 20 Scatter plot of stage delta-v versus stage mass for SLS Block 2 colored according to nozzle area ratio.

From this data set, the most desirable designs are chosen according to the single criterion of maximizing delta-v for each launch vehicle option. Table 11 displays the design variables corresponding to the NTP designs which maximize stage delta-v for both launch vehicle options.

Table 11 NTP System Design Variables Corresponding to Maximum Delta-v

Design Variable	Starship	SLS Block 2
Thrust (lb_f)	25697.000	25655.000
Reactor Power (MW)	421.990	418.350
Nozzle Area Ratio	316.370	318.740
Tank Temperature (K)	20.462	20.272
Tank Pressure (MPa)	0.153	0.156
Reactor Inlet Pressure (psi)	1476.500	1477.700
Compressor Efficiency	0.753	0.672
Turbine Efficiency	0.870	0.806
Shaft Speed (rpm)	22193.000	28597.000
Delta-v (m/s)	2586	5072

By referencing the design variables corresponding to a high-performance NTP system design generated by the surrogate models, a computer aided model was created for preliminary studies as shown in Fig. 21. A side by side comparison depicts design specifications on the left and critical components on the right. Represented in yellow, the reactor system, incorporates parameters from the Multi-Dimensional Lookup Table. Although not depicted, a detailed reactor CAD model is included within this model to reflect a more sophisticated design. The reactor core length is 48.62 inches with a reactor exterior tank diameter of 37.0 inches. The length of the turbopump assembly is approximately 18.09 inches and the nozzle area ratio is 185.22 to achieve higher performance. The CAD model also features a retractable nozzle skirt which helps the NTP system conform to the launchers' dynamic envelope constraints as discussed in the vehicle-level implication section. Although intended for preliminary analysis, the CAD model of the NTP system in Fig. 21 can indeed be integrated into the engine cluster bay with nozzles fully retracted based off the outputs of the vehicle sizing code presented in Fig. 18. Fitting into the parametric nature of this study, this CAD model can be updated to reflect the user's design point of interest.

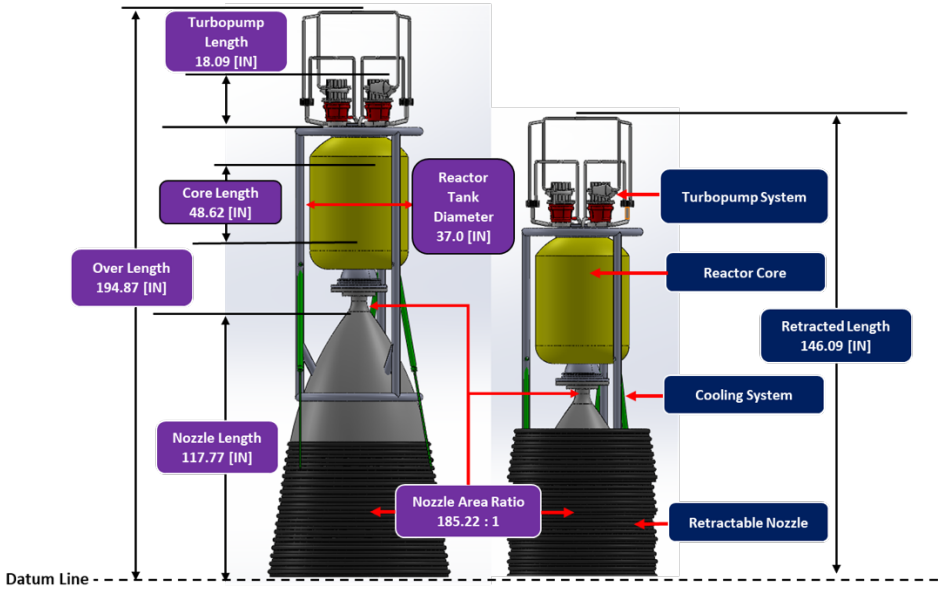

Fig. 21 CAD model of NTP system.

V. Conclusions

The work set forth in this paper develops and demonstrates a novel, coupled approach to the design space exploration of NTP systems. This approach leverages the know-how of an integrated team of subject matter experts within aerospace systems design and nuclear and radiological engineering to integrate a surrogate of nuclear reactor analysis codes within an NPSS model of an NTP system resulting in a coupled, high-fidelity model. A design of experiments was then performed on this model using bounds imposed on the design variables in order to generate surrogate models for key system responses. Using these surrogate models, tens of thousands of NTP system design

alternatives can be explored in a near-instantaneous manner, enabling rapid design space exploration. By passing the results from the design space exploration exercise for the NTP system to a vehicle sizing code, this paper also considers some baseline implications of propulsion system design on vehicle-level performance using the vehicle architecture proposed in NASA's Mars DRA 5.0.

VI. Future Work

There are many possible considerations for future work to expand the breadth of the design space exploration as compared to the baseline detailed in this paper. One such consideration would be to provide flexibility for different NTP system architectures. An instance of this could include providing the capability to explore multiple different thermodynamic cycles or consider the use of different propellant types such as Methane and Ammonia which are favorable candidates for in-situ resource utilization on Mars [22]. On the reactor side, the implementation of the multidimensional lookup table only supported the modelling of a single reactor design. While this is a step above other models for an NTP system, an important future step would be to make the NPSS model more coupled by capturing various reactor design parameter as inputs to the interpolable lookup table or by some other means. Doing so would further open the reach of the design space exploration by being able to fully consider reactor design and NTP system design in tandem.

Another expansion to the NPSS NTP model would be to further include the exploration of the turbomachinery design space using a software package such as AxSTREAM which allows for the multi-disciplinary design of turbomachinery. Notionally, this would require including the AxSTREAM design process into the design space exploration for each run of the NPSS model. Boundary conditions to the turbomachinery system would be passed to AxSTREAM from NPSS, AxSTREAM would then perform a turbomachinery design space exploration and select a design within the space. Finally, parameters of this selected turbomachinery design would then be passed back to the NPSS model to calculate NTP system performance. Such a procedure is illustrated in Fig. 22 and would allow for the consideration of elements specific to the turbomachinery architecture such as the number of compressor and turbine stages.

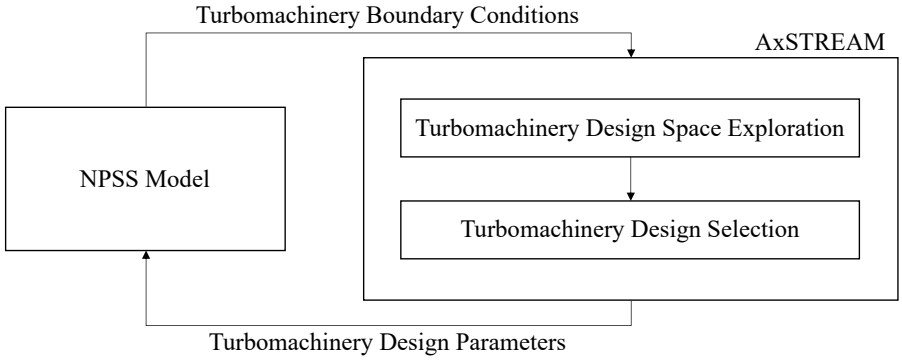

Fig. 22 Notional procedure for turbomachinery design space exploration.

Another possible capability to bring to the model would be the analysis of the system's off-design performance. NPSS would be able to support this capability through the inclusion of performance maps for the various components. Of course, performance maps would likely need to be generated through external software and codes such as AxSTREAM for the turbomachinery subsystem. Inclusion of such a capability would also require significant re-engineering of the interpolable lookup table to account for the reactor's off design performance.

While this paper represents a significant step forward by demonstrating a novel methodology for the high-fidelity analysis of NTP systems and considering first-order vehicle implications, this work represents a first step with regards to designing an entire mission utilizing an NTP propulsion system. As demonstrated by studying the vehicle-level implications of NTP system design, the goal is ultimately to be able to extend this to a full mission-level design environment. This is necessary since the conclusions and decision made at the system level must be considered within the context of the system-of-systems that it fits into. Ultimately, an extended approach to successfully build a more comprehensive NTP mission design tool would incorporate a full mission design environment that would capture not only NTP system level variables but also all the elements involved in designing an interplanetary mission.

References

[1] C. B. Reynolds, J. F. Horton, C. R. Joyner, T. Kokan, and D. J. H. Levack, "Applications of Nuclear Thermal Propulsion to Lunar Architectures," *AIAA Propuls. Energy Forum Expo. 2019*, no. August, pp. 1–17, 2019, doi: 10.2514/6.2019-4032.

[2] B. G. Drake, S. J. Hoffman, and D. W. Beaty, "Human Exploration of Mars, Design Reference Architecture 5.0," *IEEE Aerosp. Conf. Proc.*, 2010, doi: 10.1109/AERO.2010.5446736.

[3] B. W. Amiri *et al.*, "A New Capability for Nuclear Thermal Propulsion Design Recent Developments in the Recovery of SNAP-DYN Technical Data Base A New Capability for Nuclear Thermal Propulsion Design," vol. 438, no. February, 2007.

[4] S. K. Borowski, D. R. McCurdy, and T. W. Packard, "Nuclear Thermal Propulsion (NTP): A Proven, Growth Technology for 'Fast Transit' Human Missions to Mars," *AIAA Sp. 2013 Conf. Expo.*, pp. 1–20, 2013, doi: 10.2514/6.2013-5354.

[5] Luqi and G. Jacoby, "Foundations of Computer Software. Modeling, Development, and Verification of Adaptive Systems," *Lect. Notes Comput. Sci. (including Subser. Lect. Notes Artif. Intell. Lect. Notes Bioinformatics)*, vol. 6662, no. March, pp. 228–238, 2011, doi: 10.1007/978-3-642-21292-5.

[6] M. Krecicki and D. Kotlyar, "Low enriched nuclear thermal propulsion neutronic, thermal hydraulic, and system design space analysis," *Nucl. Eng. Des.*, vol. 363, Jul. 2020, doi: 10.1016/j.nucengdes.2020.110605.

[7] M. Houts and K. Aschenbrenner, "NASA's Nuclear Thermal Propulsion (NTP) Project," 2020.

[8] Southwest Research Institute, "What is Numerical Propulsion System Simulation (NPSS)?," 2019. https://www.swri.org/consortia/numerical-propulsion-system-simulation-npss.

[9] J. Leppänen, "Performance of Woodcock Delta-Tracking in Lattice Physics Applications Using the Serpent Monte Carlo Reactor Physics Burnup Calculation Code," *Ann. Nucl. Energy*, vol. 37, no. 5, pp. 715–722, 2010, doi: 10.1016/j.anucene.2010.01.011.

[10] D. A. Brown *et al.*, "ENDF/B-VIII.0: The 8th Major Release of the Nuclear Reaction Data Library with CIELO-project Cross Sections, New Standards and Thermal Scattering Data," *Nucl. Data Sheets*, vol. 148, pp. 1–142, 2018, doi: 10.1016/j.nds.2018.02.001.

[11] J. Leppänen, T. Kaltiaisenaho, V. Valtavirta, and M. Metsälä, "Development of a Coupled Neutron / Photon Transport Mode in the Serpent 2 Monte Carlo Code," *Int. Conf. Math. Comput. Methods Appl. to Nucl. Sci. Eng.*, 2017.

[12] A. E. Johnson, D. Kotlyar, S. Terlizzi, and G. Ridley, "serpentTools: A Python Package for Expediting Analysis with Serpent," *Nucl. Sci. Eng.*, pp. 1–9, Mar. 2020, doi: 10.1080/00295639.2020.1723992.

[13] M. A. Krecicki, "NEUTRONIC , THERMAL HYDRAULIC , AND SYSTEM DESIGN SPACE ANALYSIS OF A LOW ENRICHED NUCLEAR THERMAL PROPULSION ENGINE," no. December, 2019.

[14] J. Walton, "Program ELM: A Tool for Rapid Analysis of Solid-Core Nuclear Rocket," 1992.

[15] M. L. Belair, C. J. Sarmiento, and T. M. Lavelle, "Nuclear Thermal Rocket Simulation in NPSS," *49th AIAA/ASME/SAE/ASEE Jt. Propuls. Conf.*, vol. 1 PartF, pp. 1–15, 2013, doi: 10.2514/6.2013-4001.

[16] "Space Transporation System," pp. 283–336, 2004.

[17] R. Hartfield and M. Carpenter, *Similitude for Dry Liquid Rocket Engines*. 2018.

[18] S. Janarthanan, "A Statistical Model for Liquid Propellant Rocket Engine Dry Weight," 2019.

[19] F. M. Curran, C. J. Sarmiento, and B. W. Birkner, "Arcjet Nozzle Area Ratio Effects," 1990.

[20] SpaceX, "Starship User Guide," no. March, pp. 0–5, 2020, [Online]. Available: https://www.spacex.com/sites/spacex/files/starship_users_guide_v1.pdf.

[21] NASA, "Space Launch System (SLS) Mission Planner's Guide," 2018.

[22] A. Muscatello and E. Santiago-Maldonado, *Mars In Situ Resource Utilization Technology Evaluation*. 2012.